Search for exotics and test of chiral symmetry in $[c\bar{c}s\bar{s}]$ production in the continuum (final results)

Dmytro Meleshko, Elisabetta Prencipe, Sören Lange
01.10.2024

Justus-Liebig-Universität, Giessen, Germany

Belle II Germany 2024, DESY.

Impressive legacy

- Many exotic states observed in the past decade are hard to fit these spectra.
- Below $D\bar{D}/B\bar{B}$ thresholds $c\bar{c}$ and $b\bar{b}$ match potential models;

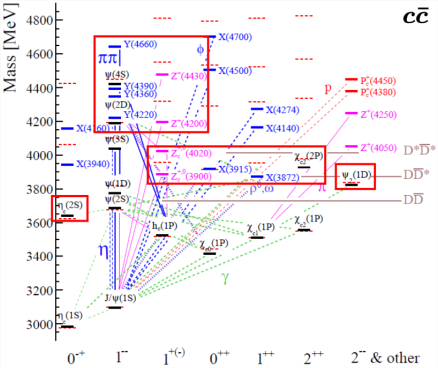

Life outside $\Upsilon(4S)$:

- Exotic XYZ states have been observed in different production mechanisms:
  - B-decays (0^+, 1^+, ...);
  - ISR (1^-);
  - $\gamma\gamma$ collisions (0^+, 2^+);
- $X(3872)$ and T_{cc}^+ have been observed in pp inclusive production at LHC. In e^+e^- collisions this would correspond to continuum production;
- 10% of data taking at Belle is 60 MeV below $\Upsilon(4S)$
- On-resonance data also contains continuum events (can be separated from B-decays by event shape);

Introduction

Invariant mass system	Decay from:	Range [GeV/c^2]
$D_s^- D_s^+$	B_s^0	[3.936 - 5.298]
$D_s^- D_s^+ \pi^0$	B_s^0	[4.071 - 5.433]
$D_s^- D_s^{*+}$	B_s^0	[4.080 - 5.433]
$D_s^- D_{s0}^*(2317)^+$	B_s^0	[4.285 - 5.433]
$J/\psi\phi$	B^0	[4.117 - 4.783]
$J/\psi\phi$	$B^\pm$	[4.117 - 4.783]
$J/\psi\phi$	continuum	all range
$D_s^- D_{s0}^*(2317)^+$, $D_s^- D_{s1}(2460)^+$, $D_s^- D_s^+ \pi^0$, $D_s^- D_s^{*+}$	continuum	all range

$B_s^0 \to D_s^{(*)+} D_s^{(*)-} \pi^0$

PhD thesis of A. Thampi

$B^{0,\pm} \to J/\Psi\phi K^{0,\pm}$

$e^+e^- \to J/\Psi\phi$ + anything

$e^+e^- \to D_s^{(*)+} D_s^{(*)-}$ + anything

$X(4274)$
$X(4685)$

$X(4630)$
$X(4500)$
$X(4700)$

LHCb results:

- 9 fb^{-1} of data
- 7 neutral X states
- 2 charged Z states

Phys. Rev. Lett. 127, 082001

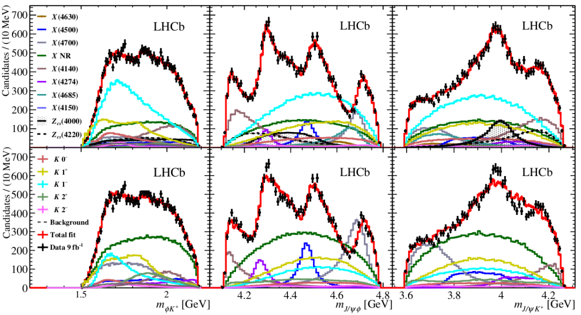

Introduction

- A Belle study reported observation of structures with the masses of $(4625.9^{+6.2}_{-6.0} \pm 0.4)$ MeV and $(4619.8^{+8.9}_{-8.0} \pm 2.3)$ MeV in the cross-section measurements of $e^+e^- \to D_s^+ D_{s1}(2536)^-$ and $e^+e^- \to D_s^+ D^*_{s2}(2573)^-$ respectively

Phys. Rev. D 100, no.11, 111103 (2019)   Phys. Rev. D 101, no.9, 091101 (2020)

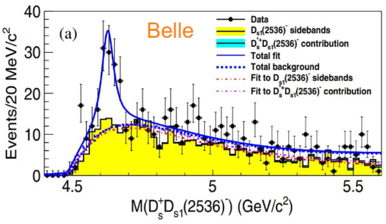

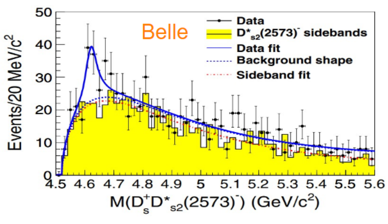

Study of $e^+e^- \to D_s^+ D_{sJ}^- A$ + c.c. at Belle

First $e^+e^- \to D_s \pi^0 X$ process studies:

- BaBar: 1267 yield on 91 fb^{-1}
- Belle: 761 yield on 87 fb^{-1}

Extrapolation from the old analysis with $D_{s0}^*(2317)$ only, but to the whole data set:

- **Belle @$\Upsilon(4S)$**: 6226 Only $D_{s0}^*(2317)$!

With one extra D_s (e.g. +3 charged tracks), efficiency is expected to drop ($< 1\%$). Around 100 events are expected on full Belle dataset.

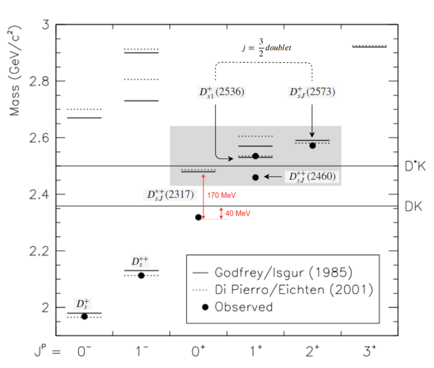

Chiral symmetry breaking test opportunity:

- $D_{s0}^*(2317)$ and $D_{s1}(2460)$ are considered as first chiral partners of the respective $c\bar{s}$ hadrons;
- The spontaneous breaking of the chiral symmetry elevates the $(0^+, 1^+)$ above the $(0^-, 1^-)$ doublet by the fixed value ΔM, which is predicted to be around 345 MeV/c^2;
- Current ΔM measurement are decades old and suffer from large systematical and statistical uncertainties;

Study of $e^+e^- \to D_s^+ D_{sJ}^- A$ + c.c. at Belle

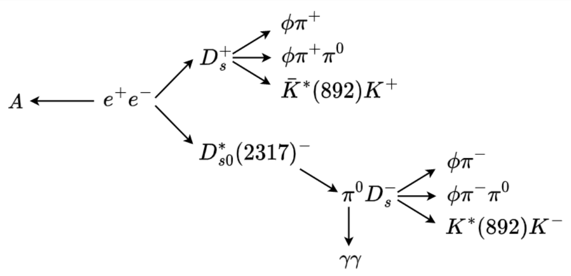

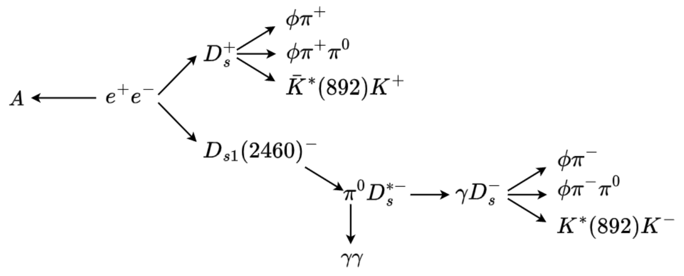

Signal MC. Optimized selection and BCS implementation.

In addition to the selection summarized on the right, the BCS selection was applied in the latest iteration of a study.

Selection optimization study has been conducted.

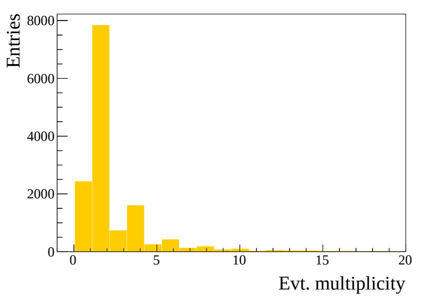

Figure 1: Signal MC. Event multiplicity before BCS application.

Particle	Selection criterion
Tracks	$dr < 0.5$ cm $dz < 3$ cm $P_{K_1}(K/\pi) > 0.5$ $P_{K_2}(K/\pi) > 0.2$ $P_{\pi}(K/\pi) < 0.9$
π^0	$E(\gamma) > 100$ MeV $p(\gamma\gamma) > 150$ MeV/c $\chi^2(\gamma\gamma) < 200$ $122 < M(\gamma\gamma) < 148$ MeV/c^2 $P_{\chi^2}(\gamma\gamma) > 1\%$
ϕ	$1.010 < M(KK) < 1.030$ GeV/c^2 $P_{\chi^2}(KK) > 0.1\%$
$K^*(892)$	$842 < M(K\pi) < 942$ MeV/c^2 $P_{\chi^2}(K\pi) > 0.1\%$
D_s	$1.9585 < M(D_s) < 1.9785$ GeV/c^2 $P_{\chi^2}(D_s) > 0.1\%$
$D_{s0}^*(2317)$	$p^*(D_s\pi^0) > 2.79$ GeV/c $P_{\chi^2}(D_s\pi^0) > 0.1\%$
Other	$\lvert cos\theta_H \rvert > 0.42$

Table 1: The summarized selection for $D_{s1}(2460)$ reconstruction.
* γ_* denotes the photon combined with D_s to create D_s^* candidate decaying into $D_s\gamma$.

The following peaking contributions are expected

$D_{sJ}(2317)^+$ invariant mass region:

- True $D_{sJ}(2317)^+$ peak
  $\sigma = (4.76 \pm 0.8)$ MeV
- $D_{sJ}(2460)^+$ reflection peak
  $\sigma = (11.8 \pm 0.3)$ MeV

$D_{sJ}(2460)^+$ invariant mass region:

- True $D_{sJ}(2460)^+$ peak
  $\sigma = (5.07 \pm 0.13)$ MeV
- $D_{sJ}(2317)^+$ reflection peak
  $\sigma = (14.6 \pm 0.7)$ MeV
- $D_{sJ}(2460)^+$ "broken signal"
  $\sigma = (16.9 \pm 1.8)$ MeV

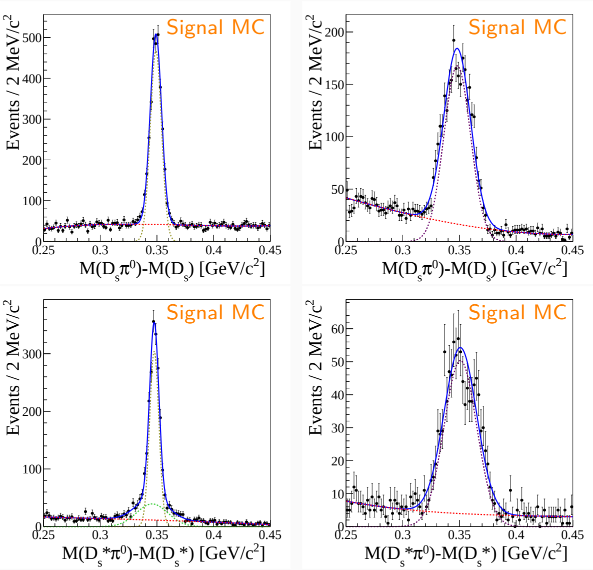

Study of $e^+e^- \to D_s^+ D_{sJ}^- A$ + c.c. at Belle

$$\Delta M(D_s\pi^0) = N_1 G(\mu_1, \sigma_1) + f^{down} N_2 G(\mu^{down}, \sigma^{down})$$
$$\Delta M(D_s^*\pi^0) = N_2 G(\mu_2, \sigma_2) + f^{up} N_1 G(\mu^{up}, \sigma^{up}) + f^{broken} N_2 G(\mu^{broken}, \sigma^{broken}) \quad (1)$$

ref: N = 3,843 ± 67, μ = 348.9 ± 0.1, σ = 6.20 ± 0.10

ref: N = 835 ± 31, μ = 347.1 ± 0.2, σ = 5.80 ± 0.20

Topology type	μ, [MeV]	σ, [MeV]	N
True $D_{s0}^*(2317)$ signal	349.3 ± 0.2	5.97± 0.25	3,797 ± 137
Feed-down background	344.8 (fixed)	13.1 (fixed)	$1.688 \cdot N_2$
True $D_{s1}(2460)$ signal	347.1 ± 0.5	5.46 ± 0.60	811 ± 155
Feed-up background	351.9 (fixed)	14.8 (fixed)	$0.134 \cdot N_1$
$D_{s1}(2460)$ broken signal	351.0 (fixed)	20.4 (fixed)	$0.247 \cdot N_2$

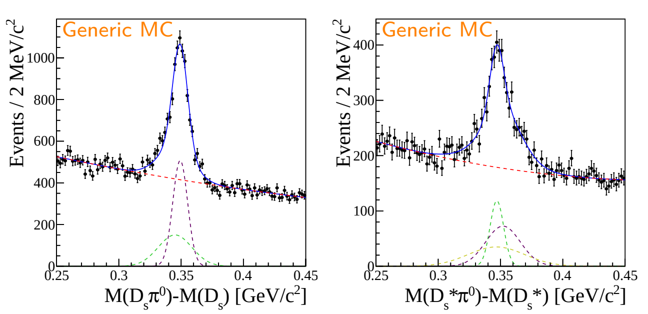

MLP application

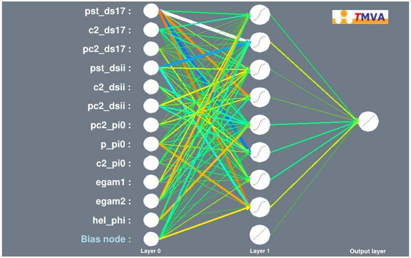

Figure 2: MLP architecture.

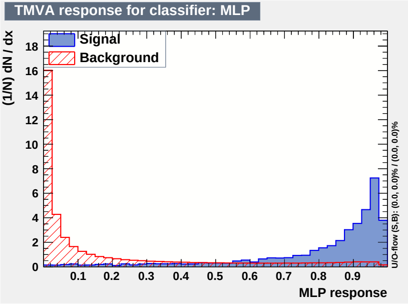

Figure 3: MLP response for classifier on training sample.

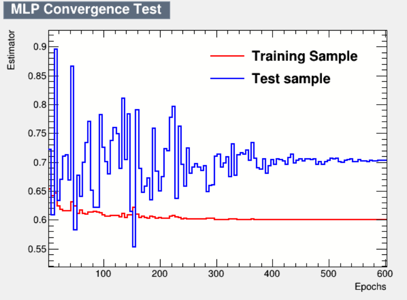

Figure 4: MLP convergence test.

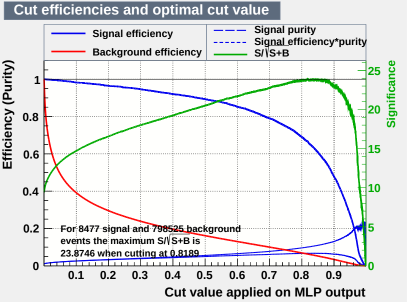

Figure 5: FoM dependence on classifier cut value.

Cut-based selection $\to$ MVA selection

Topology type	μ [MeV]	σ [MeV]	N
True $D_{s0}^*(2317)$ signal	350.0 ± 0.5	6.64 ± 0.53	688 ± 62
Feed-down background	344.8 (fixed)	13.1 (fixed)	$1.688 \cdot N_2$
True $D_{s1}(2460)$ signal	346.2 ± 1.7	6.29 ± 1.55	105 ± 27
Feed-up background	351.9 (fixed)	14.8 (fixed)	$0.134 \cdot N_1$
$D_{s1}(2460)$ broken signal	351.0 (fixed)	20.4 (fixed)	$0.247 \cdot N_2$

Cuts: $N(D_{s0}^*(2317)) = 370 \pm 45$ $N(D_{s1}(2460)) = 68 \pm 22$

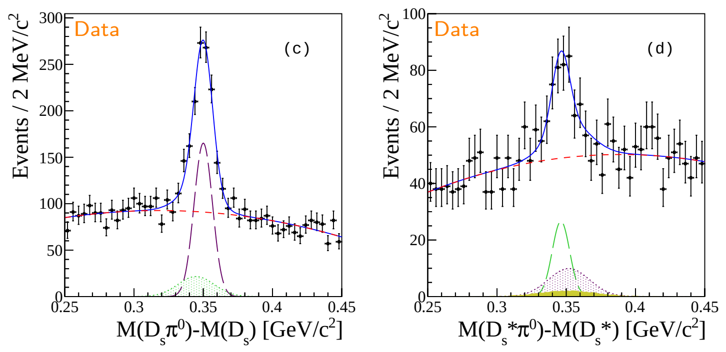

Study of $e^+e^- \to D_s^+ D_{sJ}^- A$ + c.c. at Belle

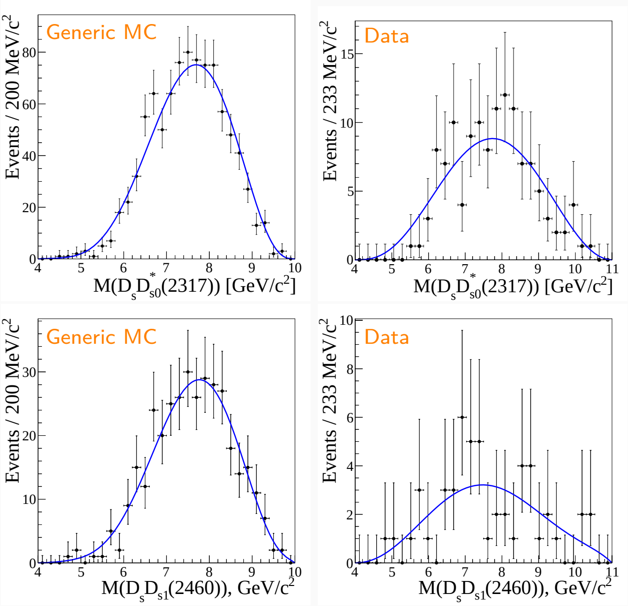

Study of $e^+e^- \to D_s^+ D_{sJ}^- A$ + c.c. at Belle

$$\frac{Br(D_{s1}(2460) \to D_s^* \pi^0)}{Br(D_{s0}^*(2317) \to D_s \pi^0)} \times \frac{\sigma(D_{s1}(2460), \mathrm{MVA})}{\sigma(D_{s0}^*(2317), \mathrm{MVA})} = 0.26 \pm 0.07(\mathrm{stat}) \pm 0.03(\mathrm{syst})$$

*The value earlier measured by Belle is $0.29 \pm 0.06 \pm 0.03$

**The value predicted by theory is 3

$$\sigma^{UL} = \frac{N^{UL} \times |1 - \Pi|^2}{\mathcal{L} \times \Sigma_{ij} \varepsilon_{ij}^* \mathcal{B}_i \mathcal{B}_j \times (1+\delta)_{ISR}}$$

Resonances	J^P	M [MeV]	Γ [MeV]	Significance
$X(4274)$	1^+	$4295 \pm 4^{+4}_{-6}$	$53 \pm 5 \pm 5$	18 (18)
$X(4685)$	1^+	$4684 \pm 7^{+13}_{-16}$	$126 \pm 15^{+37}_{-41}$	15 (15)
$X(4630)$	1^-	$4626 \pm 16^{+18}_{-110}$	$174 \pm 27^{+134}_{-73}$	5.5 (5.7)
$X(4500)$	0^+	$4474 \pm 3 \pm 3$	$77 \pm 6 \pm ^{+10}_{-8}$	20 (20)
$X(4700)$	0^+	$4694 \pm 4^{+16}_{-3}$	$87 \pm 8^{+16}_{-6}$	17 (18)

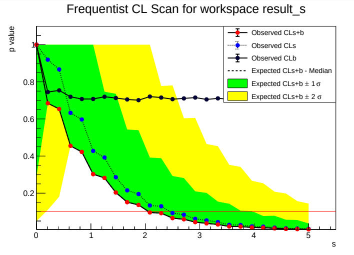

Decay chain	Total error [%]	Estimated N_{90}^{UL}	$\sigma^{UL} \times \mathcal{B}(X \to D_s D_{sJ}^*)$ [fb]
$e^+e^- \to X(4274)A$	13.3	2.45	122.5
$e^+e^- \to X(4685)A$	14.1	2.04	101.8
$e^+e^- \to X(4630)A$	18.3	2.05	228.1
$e^+e^- \to X(4500)A$	18.0	2.34	260.1
$e^+e^- \to X(4700)A$	18.7	2.18	241.8

Summary

- The process was studied on signal MC, generic MC and data;
- Cut-based and MVA selections were optimized;
- Reconstruction efficiencies are 0.42% and 0.21% for $D_s D_{s0}^*(2317)$ and $D_s D_{s1}(2460)$ decay channels with MVA selections, respectively;
- Precise mass resolution measurement:
  - $\sigma(D_{s0}^*(2317)) = 6.64 \pm 0.53$ MeV/c^2;
  - $\sigma(D_{s1}(2460)) = 6.29 \pm 1.55$ MeV/c^2;
- Precise D_{sJ} mass splitting measurement:
  - $\Delta M(D_s^*(2317)) = 350.0 \pm 0.5\,(\text{stat.}) \pm 0.1\,(\text{syst.})$ MeV/c^2
    PDG: 349.0 ± 0.6 MeV/c^2;
  - $\Delta M(D_{s1}(2460)) = 347.2 \pm 1.9\,(\text{stat.}) \pm 1.4\,(\text{syst.})$ MeV/c^2
    PDG: 347.3 ± 0.7 or 349.1 ± 0.6 MeV/c^2;
- Systematic uncertainties evaluated;
- Estimated ratio of branching fractions is consistent with earlier Belle study;
- $D_s D_{sJ}$ invariant mass distributions on data appeared to be PHSP-distributed;
- Cross-section ULs for the accessible X states are evaluated;
- For more detail, please refer to:
  - Belle Note #1585;
  - Paper Draft.

Backup

Signal MC. $D_s D_{s0}^*(2317)$ system study (threshold case).

$$\varepsilon = 0.22 \pm 0.02\%$$

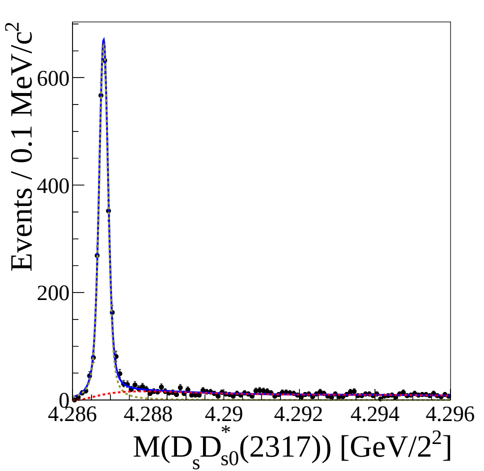

Figure 6: The $D_s D_{s0}^*(2317)$ invariant mass distribution in threshold case. The signal contribution is fitted by Voigt function, non-resonant background as approximated by the Threshold function.

MVA methods comparison

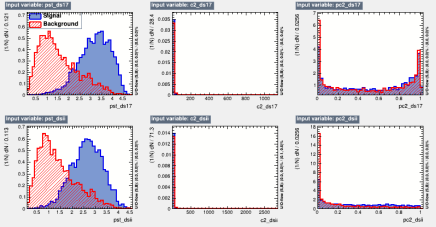

Figure 7: MVA input variables for signal (blue) and background (red) events.

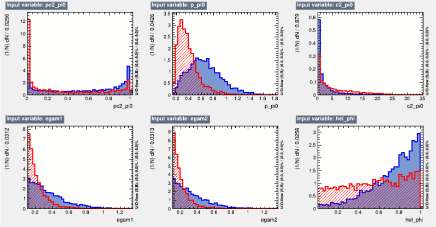

Figure 8: MVA input variables for signal (blue) and background (red) events.

- Pre-selection is applied.
- Performances of MLP, BDT, Fisher and DNN methods are compared → **MLP is chosen**
- Set of input variables is optimized with respect to correlation matrix → **redundant variables eliminated**.

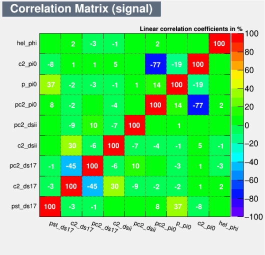

Figure 9: Input parameters Correlation Matrix for signal events.

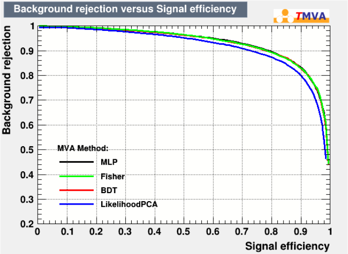

Figure 10: ROC curve.

Systematic uncertainties

Systematic Contribution	$D_s D_{s0}^*(2317)$ %	$D_s D_{s1}(2460)$ %
Charged tracks identification	3.21	3.21
Track reconstruction	2.10	2.10
MC statistics	1.82	2.42
Integrated luminosity	1.40	1.40
π^0 reconstruction	2.00	2.00
γ reconstruction	-	2.30
Secondary BF	5.83	5.62
Background fit PDF order	1.03	1.23
Mass cuts on secondary particles	5.58	7.80
TOTAL	9.50	11.22

Asymptotic method

Equation to solve:

$$\frac{\int_0^{N^{90\%}} \mathcal{L}(x)dx}{\int_0^{+\infty} \mathcal{L}(x)dx} = 0.9 \quad (2)$$

$N^{90\%}$ - wanted UL on the number of signal events.

Target dependency to study:

$$\Delta L = e^{\mathcal{L}(N_{sig}) - \mathcal{L}_0} \quad (3)$$

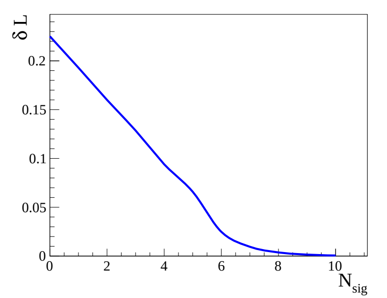

Consideration of the systematic uncertainties:

$$\Delta(\Delta L) = \frac{\Delta\mathcal{L}_j \cdot \mathcal{L}_j}{\sqrt{2\pi\varepsilon_{syst} N_j^{sig}}} \cdot e^{-\frac{1}{2}\left(\frac{\Delta N_j^{sig}}{\varepsilon_{syst} N_j^{sig}}\right)^2} \quad (4)$$

Cross-section UL calculation:

$$\sigma^{90\%} = \frac{N^{90\%}}{\varepsilon^{tot} \cdot \mathcal{L}^{int}} \quad (5)$$

CL method

Likelihood ratio:

$$\lambda(\mu) = \frac{\mathcal{L}(\mu, \hat{\hat{\theta}}|n_1, \ldots, n_{N_b})}{\mathcal{L}(\hat{\mu}, \hat{\theta}|n_1, \ldots, n_{N_b})}, \quad (6)$$

where $(\mu, \hat{\theta})$ are the parameters that maximize the likelihood for the set of observations $n_1, \ldots, n_{N_b}$; and $\hat{\hat{\theta}}$ maximizes the likelihood for a given value of μ.

Test statistics q_μ:

$$q_\mu = \begin{cases} -2ln\lambda(\mu) & \text{if } \mu > \hat{\mu}, \\ 0 & \text{otherwise} \end{cases} \quad (7)$$

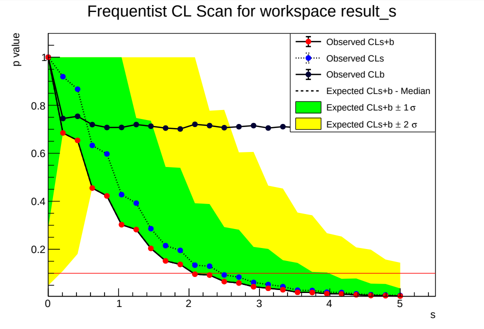

The level of agreement between the data and the hypothesized value of μ is quantified with the *p*-value:

$$p_{s+b} = P(q_\mu > q_{\mu,\text{obs}}|\mu) = \int_{\mu,\text{obs}}^{\infty} p(q_\mu|\mu) \mathrm{d}q_\mu, \quad (8)$$

where $> q_{\mu,\text{obs}}$ is the observed value of q_μ, and $p(q_\mu|\mu)$ denotes the probability density function of q_μ under the assumption of a signal strength of μ.

UL on μ at 90% CL is the largest value of μ such as p_{s+b} stays above 0.1